Received: 30 August 2019 | Accepted: 21 September 2019

DOI: 10.1002/maco.201911235

ARTICLE

Materials and Corrosion

Effect of anodizing on galvanic corrosion behavior of T300 CFRP/5083P-O Al bolted joints

Meile Shan | Kang Guo | Guoqing Gou | Zhenghong Fu | Bangjian Yang | Wei Lu

Materials Science and Engineering, Key Laboratory of Advanced Technologies of Materials, Southwest Jiaotong University, Chengdu, China

Correspondence
Guoqing Gou, School of Materials Science and Engineering, Southwest Jiaotong University, 610031 Chengdu, China.
Email: gouguoqing1001@163.com

Funding information
2018 Sichuan province science and technology program, Grant/Award Number: No. 2018HH0139

Abstract

T300 carbon fiber reinforced polymer (CFRP) and 5083P-O aluminum (5083P-O Al) alloy bolted joints have been used in high-speed trains due to the advantages of light weight and high strength. However, high potential difference between the CFRP and 5083P-O Al will induce galvanic corrosion and result in accelerating corrosion rate of 5083P-O Al, which is a potential risk for its engineering applications. In this work, combination with the electrochemical analysis, surface and cross-section corrosive morphologies analysis, the galvanic corrosion behavior between CFRP/5083P-O Al bolted joints with and without anodizing in 3.5 wt.% NaCl spray was investigated. Results indicated that severe corrosion occurred on unanodized 5083P-O Al in the coupled regions of the CFRP/5083P-O Al bolted joint due to galvanic corrosion. With the content of sulfuric acid increasing, the thickness of each Al_2O_3 layer and atomic oxygen content increases significantly. 5083P-O Al anodized by the 135 g/L H_2SO_4 + 8 g/L H_3BO_3 mixed solution had the favorable Al_2O_3 film, which increased the resistance of 5083P-O Al by roughly three orders of magnitude, effectively improving the corrosion resistance of 5083P-O Al.

KEYWORDS

5083P-O Al, anodizing, CFRP, galvanic corrosion

1 | INTRODUCTION

The application of carbon fiber reinforced polymer (CFRP) in high-speed trains has shown a tremendous rise in recent years, due to its advantages of high specific modulus, specific strength, toughness, wear resistance, and many molding processes.[1–4] In the engineering application of CFRP, it is usually necessary to be connected with metals such as 5083P-O aluminum (5083P-O Al), which is mainly used in high-speed train bodies to form a composite structure. To date, several methods have been developed for joining CFRP and metals, including adhesive bonding, welding, riveting, and bolting.[5–7] Bolting can be used for large components due to the screws can withstand high loads and repeatedly used, so CFRP is often bolted with metals in high-speed trains.

When CFRP is connected to metals, the corrosion potential of metals is usually lower than CFRP and may lead to galvanic corrosion. In general, the more noble material is protected and the less noble material experiences significantly accelerated corrosion.[5,8,9] Therefore, the study on the corrosion behavior of CFRP and metals is one of the important contents in the engineering application of CFRP.[10–12] There have been many studies on the galvanic corrosion behavior of different metals, such as Mg–Al,[13] steel–Mg [14,15] and steel–Al.[16] However, there are few studies on the

galvanic corrosion behavior of CFRP and metals, and the existing research mainly focuses on the existence of current density between CFRP/metal coupling double electrodes to illustrate that CFRP accelerates metal corrosion,[17–19] but does not provide reasonable anticorrosion measures for metal materials. Corrosion resistance of metals is a consideration in CFRP/Al bolted joints engineering applications.[20,21]

In this paper, the surface of 5083P-O Al was anodized with three different contents of sulfuric acid solution. Combination with the electrochemical analysis, surface and cross-section corrosive morphologies analysis, the galvanic corrosion behavior between CFRP/5083P-O Al bolted joints with and without anodizing in 3.5 wt.% NaCl spray was investigated.

2 | MATERIALS AND METHODS

2.1 | Materials

3 mm thickness T300 CFRP and 5083P-O Al were used in this study. T300 CFRP is made of T300 unidirectional carbon fiber (tensile strength up to 3.5 GPa) and epoxy resin, with a carbon fiber content of 70%, and 30% 5028A/5028B epoxy resin. The fiber composite laminate was covered 14 plies (ply orientation of 0°/90°). The morphologies from top view is shown in Figure 1a. The 5083P-O Al is a rolled microstructure state, chemical composition, and metallographic are respectively shown in Table 1 and Figure 1b.

2.2 | Anodizing of 5083P-O Al

Al_2O_3 layers were produced on 5083P-O Al in three different concentrations of sulfuric acid by anodization. The anodizing process is shown in Figure 2. All the specimen surfaces were ultrasonically cleaned in deionized water for 10 min to remove the surface stains. Before the anodization, the pretreated specimen was sonicated in a 20 g/L NaOH solution for 1 min, sonicated in 30% HNO_3 for 5 s to expose a fresh surface, ultrasonically washed with water and dried to perform anodization.[22,23] Then the specimens were anodized at 15 V voltage for 40 min at three concentration parameters: 45 g/L H_2SO_4 + 8 g/L H_3BO_3, 90 g/L H_2SO_4 + 8 g/L H_3BO_3, and 135 g/L H_2SO_4 + 8 g/L H_3BO_3. After anodizing, the cross-section and surface morphologies were imaged by scanning electron microscope (SEM). The chemical composition of the oxide layers was analyzed by EDS.

2.3 | Electrochemical test

To determine the electrochemical properties, the T300 CFRP and 5083P-O Al (unanodized and anodized) were cut into 10 × 10 × 3 mm rectangular parallelepiped specimens. The 5083P-O Al surface had no passivation film, and the surface of the CFRP was exposed with carbon fiber to lead the copper wire from the surface. Except for the working surface, the rest was partially packaged with denture base resin and denture-based resin liquid. After being fully cured, the samples were polished one by one with #180, #400, #600, #800, #1,000, #1,200, #1,500 sandpaper, rinsed with deionized water, then washed with alcohol and acetone. Electrochemical tests were conducted in a three-electrode flat cell. A saturated calomel electrode and a platinum mesh were used as the reference and counter electrodes and the specimens as working electrode.[24,25] The test solution was 3.5 wt.% NaCl and the pH was 5. Before polarization, specimens were immersed in the solution for 30 min to allow the system to reach steady state. The polarization measurements were performed with respect to the open circuit potential −500 to 500 mV at a scan rate of 1 mV/s. EIS was carried out at frequency ranged between 10^{-2} and 10^5 Hz. ECN was applied to analyze the galvanic corrosion between CFRP and 5083P-O A1 for 24 hr.

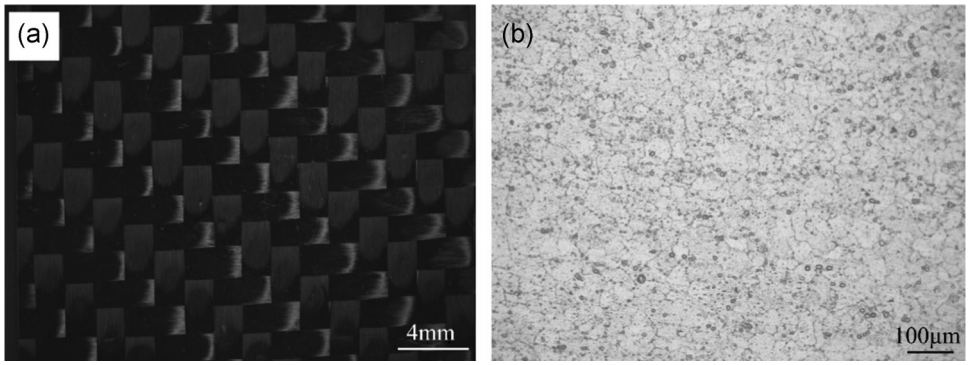

FIGURE 1 Metallographic picture of (a) T300 carbon fiber reinforced polymer and (b) 5083P-O aluminum

TABLE 1 Chemical composition of 5083P-O aluminum (wt.%)

Si	Cu	Mg	Zn	Mn	Ti	Cr	Fe	Al
≤0.40	≤0.10	4.0–4.9	≤0.25	0.40–1.0	≤0.15	0.05–0.25	0.00–0.40	Bal

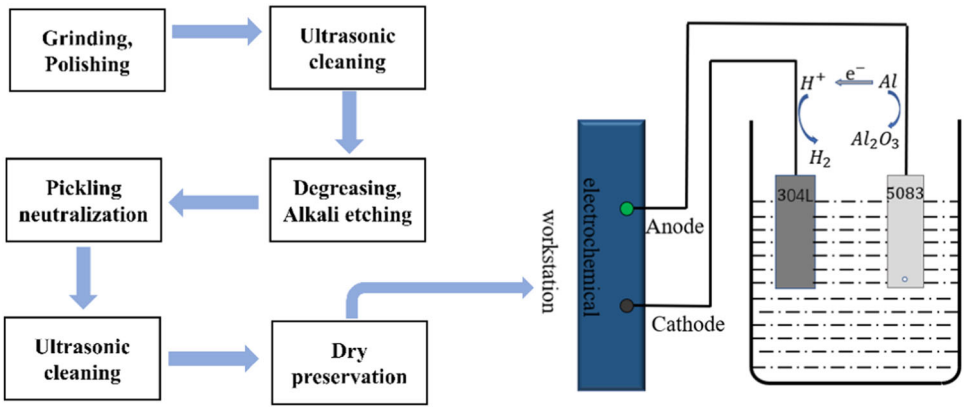

FIGURE 2 Anodizing process [Color figure can be viewed at wileyonlinelibrary.com]

2.4 | Salt spray test

The salt spray test is used to observe the corrosion morphology of CFRP/5083P-O Al bolted joints after long-term exposure to corrosive medium. Before the salt spray test, 30 × 100 × 3 mm CFRPs, 5083P-O Al (anodized and unanodized) were prepared, and CFRP was bolted to the aluminum alloys with a torque of 20 N·m. Figure 3 depicts the geometry of the bolted joint with an overlap area of 40 × 30 mm and a hole diameter of 6 mm. The bolted joints were exposed under salt spray environment condition (3.5 wt.% NaCl solutions, pH 5) at a temperature of 35°C in a salt spray chamber. After continuous spraying for 336 hr, the samples were cleaned according to ASTM B117 and the surface topography of the bolted joints was observed by a stereomicroscope and SEM.

3 | RESULTS AND DISCUSSION

3.1 | Anodizing results

Figure 4a–c shows cross-sections of oxide films on anodized 5083P-O Al with three mixed electrolytes: 45 g/L H_2SO_4 + 8 g/L H_3BO_3, 90 g/L H_2SO_4 + 8 g/L H_3BO_3, and 135 g/L H_2SO_4 + 8 g/L H_3BO_3, and the chemical composition is shown in Table 2. The concentration of sulfuric acid in the anodizing solution caused a significant difference in the thickness of the oxide layer. As the content of sulfuric acid increases, the thickness of Al_2O_3 layer and atomic oxygen content increases significantly. The coating thicknesses of #1 45 g/L H_2SO_4 + 8 g/L H_3BO_3, #2 90 g/L H_2SO_4 + 8 g/L H_3BO_3, and #3 135 g/L H_2SO_4 + 8 g/L H_3BO_3 are 5.50, 9.06, and

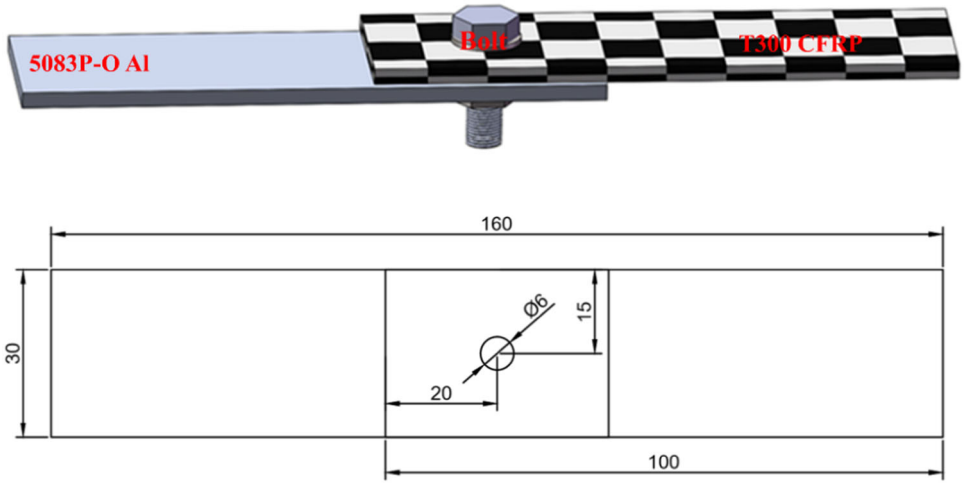

FIGURE 3 Specimen geometry used in salt spray test. 5083P-O Al, 5083P-O aluminum; CFRP, carbon fiber reinforced polymer [Color figure can be viewed at wileyonlinelibrary.com]

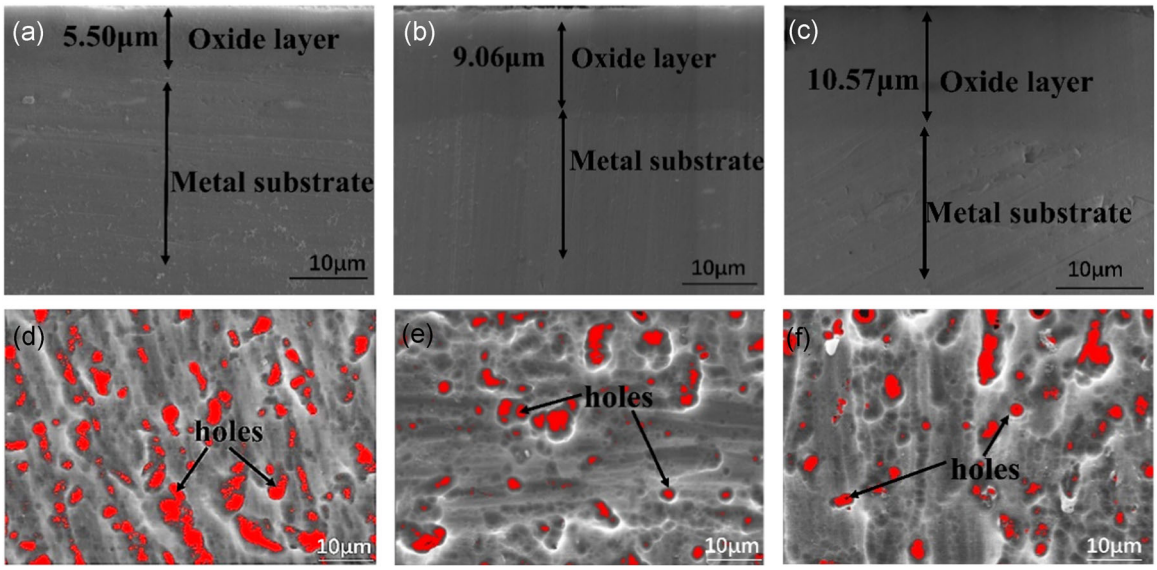

FIGURE 4 Cross-section of the specimen (a) #1 anodized specimen, (b) #2 anodized specimen and (c) #3 anodized specimen. Surface of the specimen under scanning electron microscope for (d) #1 anodized specimen, (e) #2 anodized specimen and (f) #3 anodized specimen [Color figure can be viewed at wileyonlinelibrary.com]

10.57 μm, respectively. Figure 4d–f are the surface topography of the coating, the red area indicates the pore size, as the concentration of sulfuric acid increases, the number of pores formed on the surface of the coating becomes lower and the coating is denser. The increase of sulfuric acid concentration increases the anodic oxidation current density, and accelerates the ion movement, resulting in the faster formation of the film and greater thickness of the film.

3.2 | Polarization curve and EIS

The polarization curve of the materials measured by the potentiodynamic scanning is shown in Figure 5a. CFRP has the highest self-corrosion potential (−0.15 V), and 5083P-O Al has a lower self-corrosion potential (−0.8 V). According to Schneider et al.,[26] if the potential difference between two materials is higher than 0.05 V, the effect of galvanic corrosion should not be neglected. In this study, the potential difference between CFRP and 5083P-O Al can reach 0.65 V, which means that when the CFRP is in contact with the Al the galvanic corrosion effect will be very serious. The self-corrosion rate of the specimens calculated from the anodic/cathodic Tafel slope are shown in Figure 5b, as the concentration of sulfuric acid in the anodizing solution increases, the self-corrosion rate of 5083P-O Al decreases. Unanodized 5083P-O Al has the fastest self-corrosion rate (4.45×10^{-2} mm/a), and specimen anodized by 135 g/L H_2SO_4 + 8 g/L H_3BO_3 has the lowest self-corrosion rate (4.43×10^{-4} mm/a), which is two orders of magnitude lower than unanodized 5083P-O Al. Anodization reduces the corrosion current and corrosion rate, improves the corrosion resistance of 5083P-O Al, and the thicker the anodic oxide film, the better the corrosion resistance.

TABLE 2 Analysis of chemical composition of Al_2O_3 layers

Specimen	Atomic aluminum content (%)	Atomic oxygen content (%)
5083P-O Al	95.60	4.40
45 g/L H_2SO_4 + 8 g/L H_3BO_3	43.55	56.45
90 g/L H_2SO_4 + 8 g/L H_3BO_3	39.50	60.60
135 g/L H_2SO_4 + 8 g/L H_3BO_3	36.51	63.49

Abbreviation: 5083P-O Al, 5083P-O aluminum.

Figure 6 shows the EIS analysis results; all Nyquist diagrams only show a capacitive reactance arc. According to the electrochemical impedance test principle,[27] the radius of the capacitive anti-arc in the Nyquist diagram reflects the surface polarization resistance of the material, and the larger the radius of the arc resistance of the capacitor, the better the corrosion resistance. We can see that as the concentration of sulfuric acid in the anodizing solution increases, the capacitive anti-arc increases gradually. Bode diagrams (Figure 6b) are similar to the Nyquist diagram, the impedance modulus of the anodized specimens is significantly higher than the impedance modulus of the 5083P-O Al without anodization, in which the impedance modulus of specimen anodized by 135 g/L H_2SO_4 + 8 g/L H_3BO_3 is the highest, 10 times

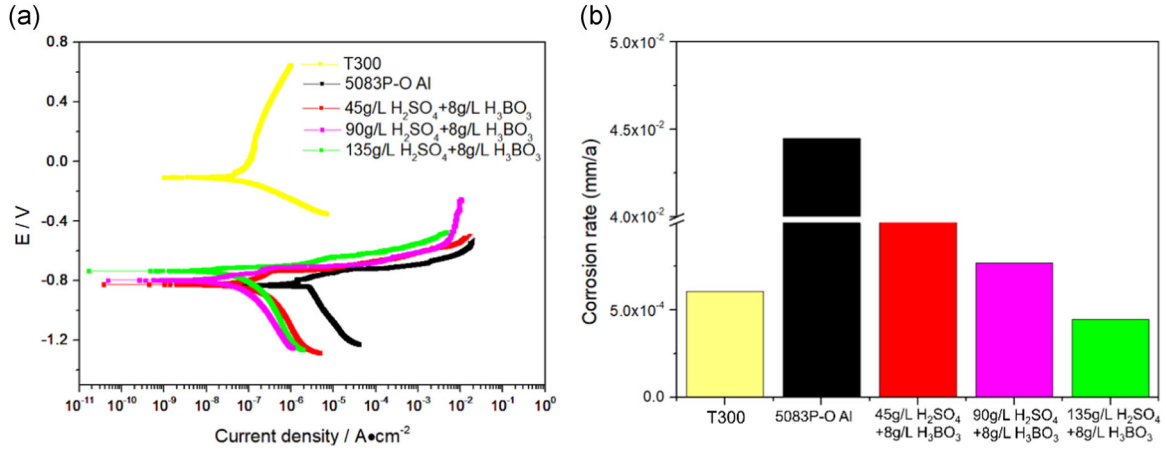

FIGURE 5 (a) Polarization curve in 3.5% NaCl solution. (b) Corrosion rate of materials [Color figure can be viewed at wileyonlinelibrary.com]

than the unanodized 5083P-O Al. Table 3 shows the fitted electrochemical parameters of the EIS spectra of CFRP and 5083P-O Al, where R_s is the solution resistance, CPE-T is the interfacial capacitance, CPE-P is the diffusion index of the curve and R_p is a polarization resistance. It can be seen from Table 3 and Figure 6d that the R_p of the CFRP is much larger than 5083P-O Al, at the same time, and the R_p of anodized 5083P-O Al by anodizing is three orders of magnitude higher than that of unanodized 5083P-O Al.

3.3 | Galvanic corrosion test results

The galvanic current curves between CFRP and 5083P-O Al (unanodized and anodized) are shown in Figure 7. The results show that the galvanic current density of

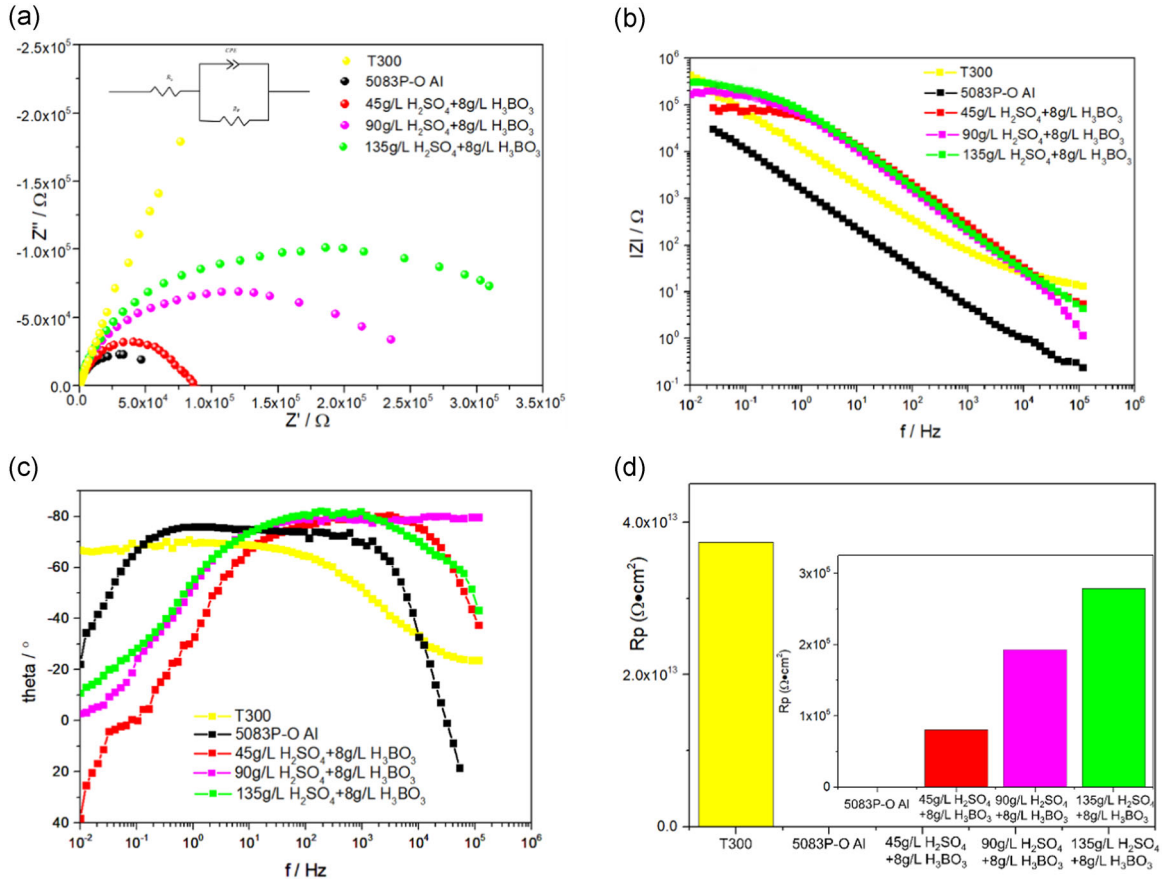

FIGURE 6 (a) Nyquist plot, (b) Bode plot, (c) Bode plot and (d) column diagram of R_p [Color figure can be viewed at wileyonlinelibrary.com]

TABLE 3 Parameters of electrochemical impedance

Material	R_s ($\Omega \cdot cm^2$)	CPE-T ($\mu F \cdot cm^2$)	CPE-P	R_p ($\Omega \cdot cm^2$)
T300	15.89	2.21×10^{-5}	0.75	3.74×10^{13}
5083P-O Al	0.99	1.20×10^{-6}	0.91	336.90
45 g/L H_2SO_4 + 8 g/L H_3BO_3	0.47	4.19×10^{-7}	1.0	8.07×10^{4}
90 g/L H_2SO_4 + 8 g/L H_3BO_3	1.17	2.79×10^{-6}	0.88	1.93×10^{5}
135 g/L H_2SO_4 + 8 g/L H_3BO_3	2.75	2.25×10^{-6}	0.87	2.79×10^{5}

Abbreviation: 5083P-O Al, 5083P-O aluminum.

CFRP/5083P-O Al anodized by 45 g/L H_2SO_4 + 8 g/L H_3BO_3 coupling fluctuates greatly, which is the same as that of CFRP/unanodized 5083P-O Al coupling. There are many sharp transient peaks in the current, indicating that the corrosion reaction is happening rapidly. However, the galvanic current density and current peak density of CFRP/5083P-O Al (anodized by 90 g/L H_2SO_4 + 8 g/L H_3BO_3) coupling and CFRP/5083P-O Al (anodized by 135 g/L H_2SO_4 + 8 g/L H_3BO_3) coupling decreased, indicating that the reaction speed is slow at this time.[28] The sample anodized by 135 g/L H_2SO_4 + 8 g/L H_3BO_3 has the best anticorrosion effect, because the galvanic corrosion current density is <5 $\mu A/cm^2$.

Figure 8a shows that the surface of the unanodized 5083P-O Al specimen was severely corroded, the oxide film on the surface of the specimen was cracked, and large pitting pits appeared. The surface of anodized specimens was not seriously corroded, and the number of pitting pits decreased as the thickness of the oxide film increased. However, several cracks occurred in the oxide film at the grain boundary because the anodic oxide film at grain boundaries is weak, so it is relatively easy to be damaged by chloride ions during the process of dissolution and destruction. As shown in Figure 8g, because the oxide film was uniform and continuous, corrosion pitting did not occur in the specimen anodized by 135 g/L H_2SO_4 + 8 g/L H_3BO_3. When the anodized 5083P-O Al is connected with the CFRP, the aluminum oxide film layer is first destroyed, which serves to protect the aluminum matrix. As shown in Figure 9b,d,f,h, the CFRP coupled with unanodized 5083P-O Al has no obvious defects on the surface due to the protection of galvanic effect. However, the CFRP coupled with the anodized 5083P-O Al has defects such as cracks and holes. Anodizing improves the corrosion resistance of the 5083P-O Al and promotes a more uniform corrosion between the CFRP/5083P-O Al bolted joints, which effectively avoids serious damage of the negative potential metal material.

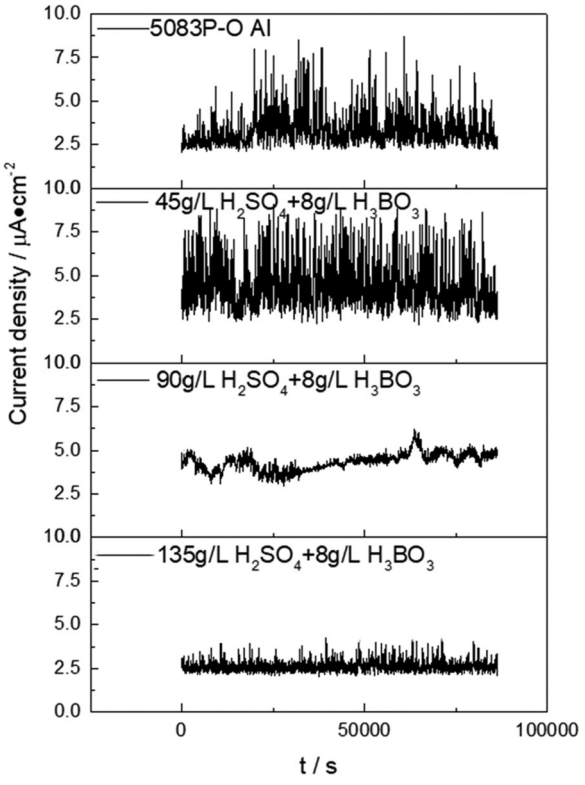

FIGURE 7 Galvanic current densities of carbon fiber reinforced polymer/5083P-O aluminum couples

3.4 | Salt spray corrosion results

Figure 9 shows the morphology of the CFRP/5083P-O Al bolted joints after 336 hr of salt spray corrosion. More severe corrosion occurred on the unanodized 5083P-O Al, a large number of pits appeared in the uncoupled regions, and the pits in the coupling region expanded and connected into a sheet. The corrosion diagram of CFRP/5083P-O Al (anodized by 45 g/L H_2SO_4 + 8 g/L H_3BO_3) bolted joints shows that part of the oxide film fell off in the coupling region, and there were a small amount pits on the surface of the sample. In the macro and micro images, no obvious pits were observed for CFRP/5083P-O Al bolted (anodized by 90 g/L H_2SO_4 + 8 g/L H_3BO_3) joints and the CFEP/5083P-O Al (anodized by 135 g/L H_2SO_4 + 8 g/L H_3BO_3) bolted joints. The anodized 5083P-O Al anodized layer conforms to the standard specification MILA8625F, and the number of pits per 150 square inches of test material is less than 15.

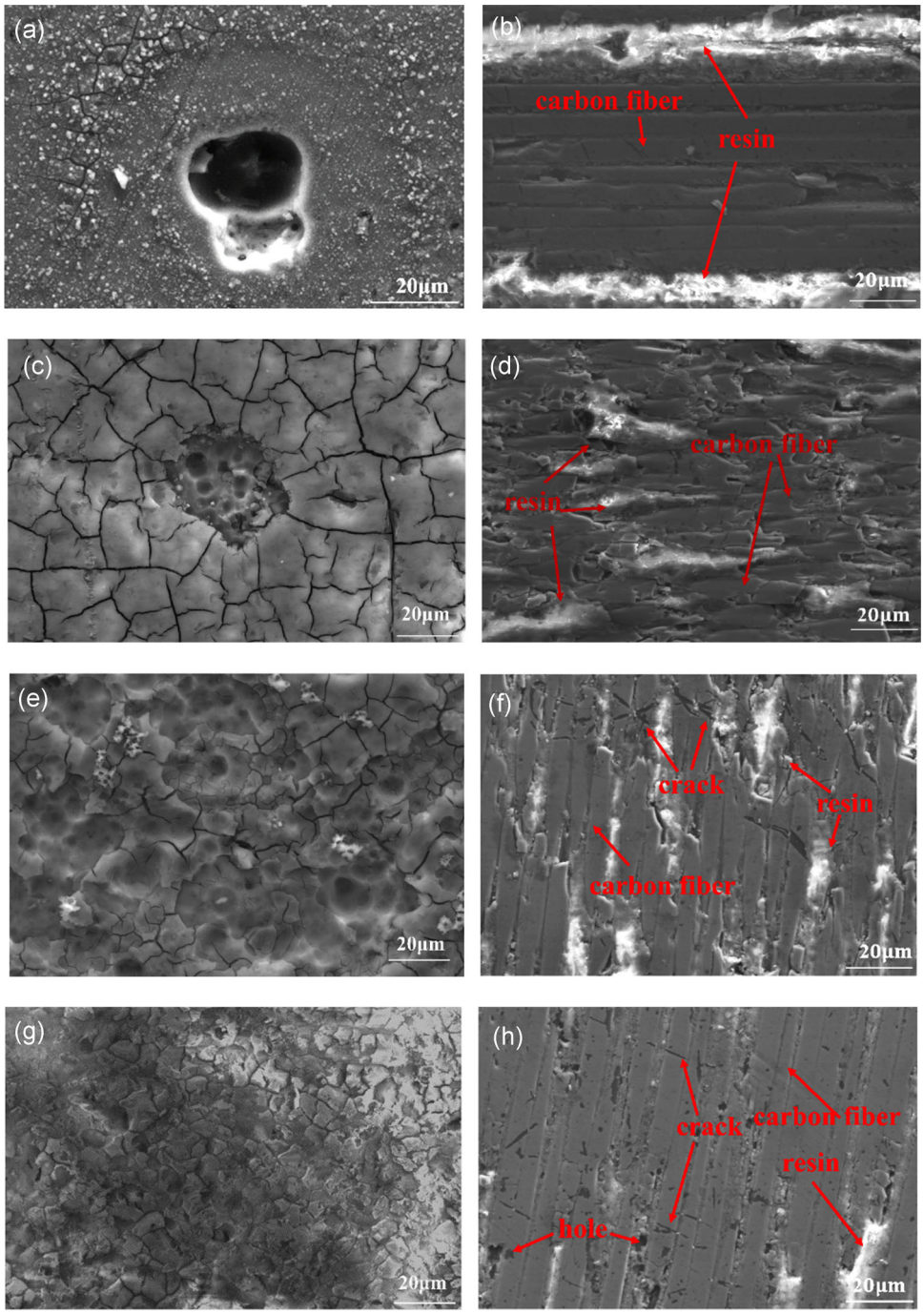

FIGURE 8 Surface of the specimen under scanning electron microscope: (a) unanodized 5083P-O Al, (b) CFRP coupled specimen, (c) specimen anodized by 45 g/L H_2SO_4 + 8 g/L H_3BO_3, (d) CFRP coupled specimen, (e) specimen anodized by 90 g/L H_2SO_4 + 8 g/L H_3BO_3, (f) CFRP coupled specimen, (g) specimen anodized by 135 g/L H_2SO_4 + 8 g/L H_3BO_3 and (h) CFRP coupled specimen. 5083P-O Al, 5083P-O aluminum; CFRP, carbon fiber reinforced polymer [Color figure can be viewed at wileyonlinelibrary.com]

The cross-section of corrosion specimens is shown in Figure 10; unanodized 5083P-O Al has the most serious corrosion, and the depth of the corrosion pit is 30 times of the specimen anodized by 45 g/L H_2SO_4 + 8 g/L H_3BO_3, the oxidation film of specimen anodized by 90 g/L H_2SO_4 + 8 g/L H_3BO_3 and specimen anodized by 135 g/L H_2SO_4 + 8 g/L H_3BO_3 basically has no obvious corrosion pit.

3.5 | Discussion

Combined with the results of electrochemical and salt spray tests, the corrosion mechanism of CFRP/5083P-O Al in 3.5 wt.% NaCl dielectric solution was proposed. In the galvanic corrosion process (Figure 11), when the CFRP is coupled with the 5083P-O Al, the CFRP acts as a cathode, does not

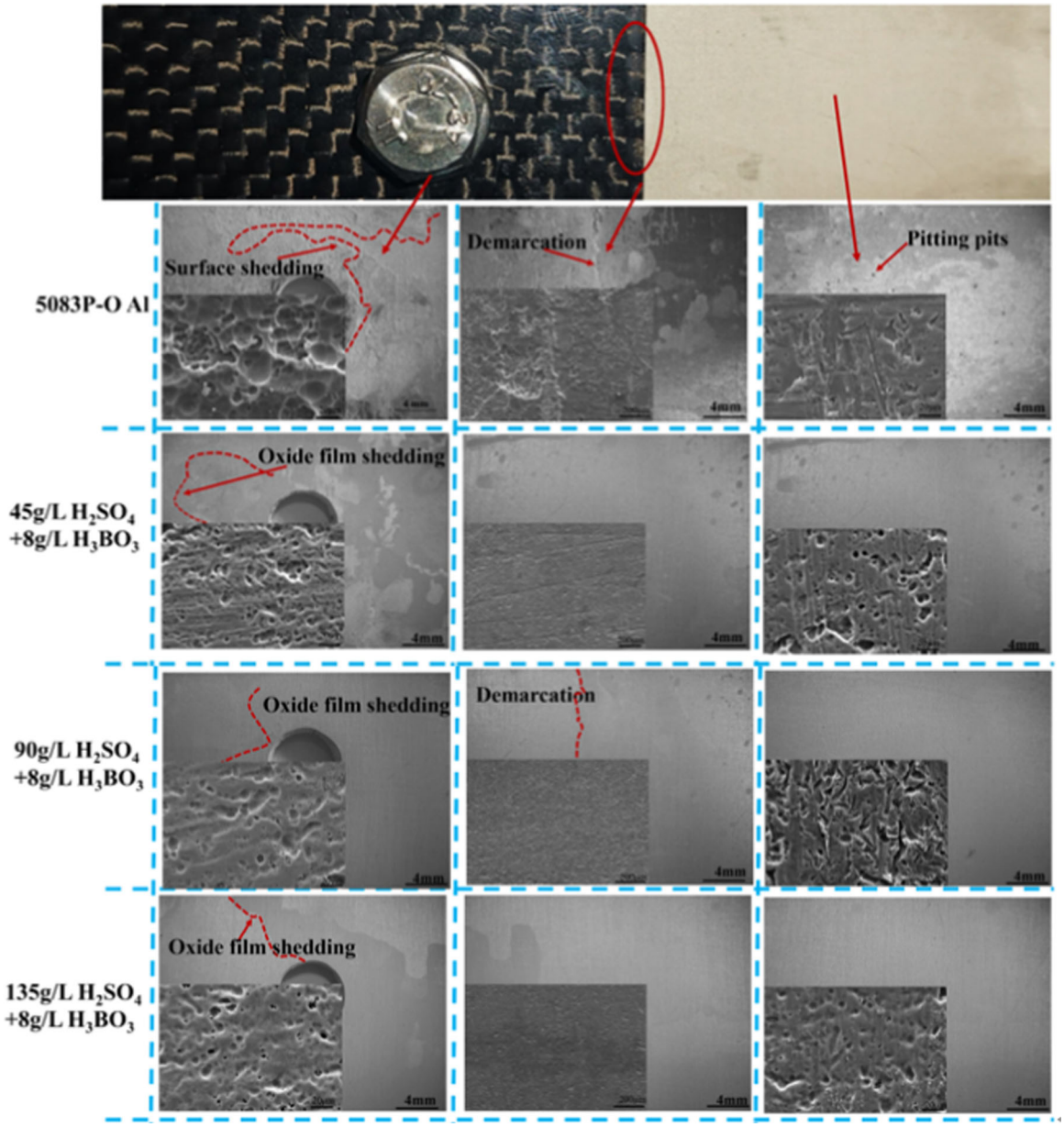

FIGURE 9 Corrosion morphology of bolted joints. 5083P-O Al, 5083P-O aluminum [Color figure can be viewed at wileyonlinelibrary.com]

participate in the reaction, the electrode oxygen undergoes reduction reaction, and the reaction formula is

$$O_2 + 2H_2O + 4e^- = 4OH^-. \quad (1)$$

The Al coupled with the CFRP acts as an anode, the surface loses electrons, and an oxidation reaction occurs to form an oxide. The reaction formula is

$$Al = Al^{3+} + 3e^-. \quad (2)$$

In the electrolyte solution, the potential difference between the two materials causes the electrons to flow between the two electrodes. Al^{3+} is easily hydrolyzed to produce a large amount of H^+, forming $Al(OH)_3$ which is difficult to dissolve in water. The reaction formula is

$$Al^{3+} + 3H_2O \rightarrow Al(OH)_3 \downarrow + 3H^+. \quad (3)$$

The deposition of $Al(OH)_3$ will create an occlusion environment to prevent the entry of dissolved oxygen. To maintain the electrical neutrality of the local environment, Cl^- is continuously moved and undergoes a series of reactions with the oxidation film. Subsequently, Cl^- diffuses to the surface of the base aluminum alloy, transforming the metal into an activated state, then the metal is dissolved by

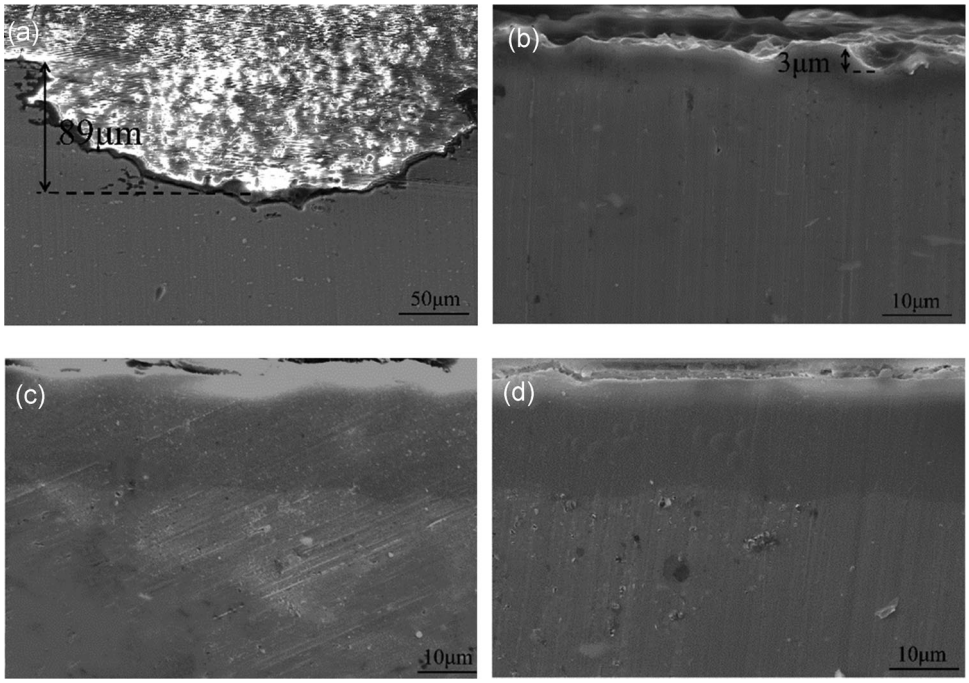

FIGURE 10 Cross-section of the aluminum alloy after corrosion (a) unanodized 5083P-O Al, (b) specimen anodized by 45 g/L H_2SO_4 + 8 g/L H_3BO_3, (c) specimen anodized by 90 g/L H_2SO_4 + 8 g/L H_3BO_3 and (d) specimen anodized by 135 g/L H_2SO_4 + 8 g/L H_3BO_3. 5083P-O Al, 5083P-O aluminum

anodic reaction and pores appear. The metal in the pores is continuously dissolved, forming high concentration chlorides (such as $AlCl_3$), causing the H^+ concentration to increase one more time. Under the action of high Cl^- concentration and low pH, an acidic solution with extremely low pH and high corrosivity is formed in the pores. The metal dissolution in the pores accelerates, and the pores develop and extend rapidly, which accelerates the corrosion of 5083P-O Al. Al_2O_3 films of different thicknesses can act as barrier layers to hinder reactions (1), (2) and (3). The corrosion resistance of the anodized 5083P-O Al samples is significantly improved because the oxide film is thicker than the passivation film formed on the Al surface in the natural state. The thicker the oxide film, the slower the diffusion of Cl^- to the surface of the base aluminum alloy, thus reducing the metal dissolution rate and improving the corrosion resistance.

4 | CONCLUSION

The 5083P-O Al was anodized by three different sulfuric acid concentrations. The corrosion behavior and mechanism of CFRP/5083P-O Al were studied by electrochemical corrosion and salt spray test. The results are as follows:

1. 5083P-O Al was anodized by three concentrations of sulfuric acid: 45 g/L H_2SO_4 + 8 g/L H_3BO_3, 90 g/L H_2SO_4 + 8 g/L H_3BO_3 and 135 g/L H_2SO_4 + 8 g/L H_3BO_3. The results showed that as the concentration of sulfuric acid increased, the anodic oxidation film on the surface of 5083 P-O Al became thicker, and the thickness of 135 g/L H_2SO_4 + 8 g/L H_3BO_3 coating was up to 10.57 μm.

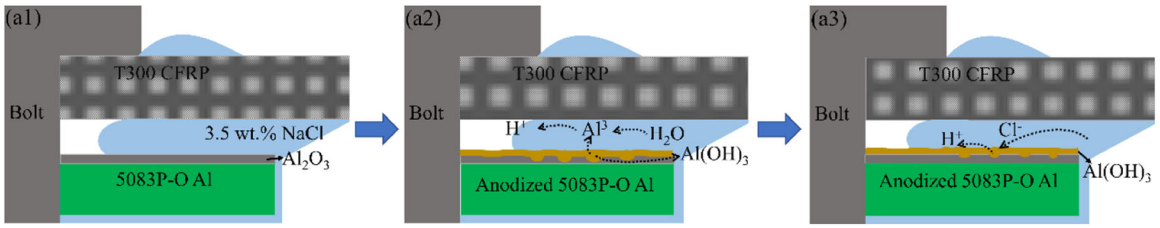

FIGURE 11 Schematic representation of the galvanic corrosion processes in the CFRP/5083P-O Al (a1 through a3) bolted joints. 5083P-O Al, 5083P-O aluminum; CFRP, carbon fiber reinforced polymer [Color figure can be viewed at wileyonlinelibrary.com]

2. The galvanic effect accelerates the corrosion rate of 5083P-O Al. The thicker the oxide film, the more difficult the diffusion of Cl^- in the electrolyte solution is, and the more significant the corrosion resistance of 5083P-O Al is.
3. In this study, all bolted joints were observed after 336 hr of salt spray test. The 135 g/L H_2SO_4 + 8 g/L H_3BO_3 mixed solution anodized layer meets the standard MILA8625F to improve the corrosion resistance of 5083P-O Al.

ACKNOWLEDGEMENT

The authors acknowledge the financial support from the 2018 Sichuan province science and technology program (No. 2018HH0139).

ORCID

Guoqing Gou http://orcid.org/0000-0003-1559-3059

REFERENCES

[1] C. Batuwitage, S. Fawzia, D. Thambiratnam, R. Al-Mahaidi, *Compos. Struct.* **2017**, *160*, 1287.
[2] F. Bellucci, A. Di Martino, C. Liberti, *J. Appl. Electrochem.* **1986**, *16*, 15.
[3] J. Ren, K. Li, S. Zhang, *Mater. Des.* **2015**, *65*, 174.
[4] X. Wu, J. Sun, J. Wang, Y. Jiang, J. Li, *Mater. Corros.* **2019**, *70*, 1036.
[5] S. Li, H. A. Khan, L. H. Hihara, H. Cong, J. Li, *Corros. Sci.* **2018**, *132*, 300.
[6] H. Y. Yu, H. Xu, C. X. Zhou, *Nat. Sci* **2016**, *44*, 1729.
[7] J. Hu, K. Zhang, Q. Yang, H. Cheng, S. Liu, Y. Yang, *Mater. Des.* **2017**, *134*, 91.
[8] H. G. Son, Y. B. Park, J. H. Kweon, J. H. Choi, *Compos. Struct.* **2014**, *108*, 151.
[9] W. Hufenbach, L. A. Dobrzański, M. Gude, J. Konieczny, *J. Achi. Mater. Manuf. Eng.* **2007**, *20*, 119.
[10] R. Ireland, L. Arronche, V. La Saponara, *Composites, Part B* **2012**, *43*, 183.
[11] Z. Peng, X. Nie, *Surf. Coat. Technol.* **2013**, *215*, 85.
[12] F. Lu, X. Zhang, M. Liu, *J. Chin. Soc. Corros. Prot.* **2005**, *1*, 39.
[13] A. Pardo, P. Casajús, M. Mohedano, A. E. Coy, F. Viejo, B. Torres, E. Matykina, *Appl. Surf. Sci.* **2009**, *255*, 6968.
[14] F. Andreatta, J. Rodriguez, M. Mouanga, A. Lanzutti, L. Fedrizzi, M. G. Olivier, *Mater. Corros.* **2019**, *70*, 793.
[15] I. Adlakha, B. G. Bazehhour, N. C. Muthegowda, K. N. Solanki, *Corros. Sci.* **2018**, *133*, 300.
[16] P. Du, J. Z. Li, Y. L. Zhao, Y. G. Dai, Z. D. Yang, Y. W. Tian, *Int. J. Electrochem. Sci.* **2018**, *13*, 11164.
[17] Y. Pan, G. Wu, X. Cheng, Z. Zhang, M. Li, S. Ji, *Corros. Sci.* **2015**, *98*, 672.
[18] C. Zhang, D. J. Zheng, G. L. Song, *Acta Metall. Sin. (Engl. Lett.)* **2017**, *304*, 342.
[19] L. Arronche, K. Gordon, D. Ryu, V. La Saponara, L. Cheng, *J. Mater. Sci.* **2013**, *48*, 1315.
[20] S. A. Abdel-Gawad, W. M. Osman, A. M. Fekry, *Surf. Interfaces* **2019**, *14*, 314.
[21] M. I. Tawakkal, A. K. Akhmad, presented at J. Phys. Bandung, Indonesia, August 29–31, **2019**.
[22] M. Kocabaş, C. Örnek, M. Curioni, N. Cansever, *Surf. Coat. Technol.* **2019**, *364*, 231.
[23] Y. Zhang, T. Lin, *Colloids Surf., A* **2019**, *568*, 43.
[24] L. Hamill, D. C. Hofmann, S. Nutt, *Adv. Eng. Mater.* **2018**, *20*, 1700711.
[25] F. Lionetto, C. Mele, P. Leo, S. D'Ostuni, F. Balle, *Composites, Part B* **2018**, *144*, 134.
[26] M. Schneider, K. Kremmer, C. Lämmel, K. Sempf, M. Herrmann, *Corros. Sci.* **2014**, *80*, 191.
[27] M. Songür, H. Çelikkan, F. Gökmeşe, S. A. Şimşek, N. Ş. Altun, M. L. Aksu, *J. Appl. Electrochem.* **2009**, *39*, 1259.
[28] J. Hu, *Ph.D. Thesis*, Southwest Jiaotong University (China), **2018**.

How to cite this article: Shan M, Guo K, Gou G, Fu Z, Yang B, Lu W. Effect of anodizing on galvanic corrosion behavior of T300 CFRP/5083P-O Al bolted joints. *Materials and Corrosion*. 2019;1–10. https://doi.org/10.1002/maco.201911235